ACS OMEGA

Article

Cite This: ACS Omega 2019, 4, 8874−8880

http://pubs.acs.org/journal/acsodf

Thiophene Derivatives as New Anticancer Agents and Their Therapeutic Delivery Using Folate Receptor-Targeting Nanocarriers

Menghui Zhao,[†] Yaxin Cui,[†] Lang Zhao,[§] Tianyu Zhu,[†] Robert J. Lee,[†,‡] Weiwei Liao,[§] Fengying Sun,[†] Youxin Li,*[,†] and Lesheng Teng*[,†]

[†]School of Life Sciences and [§]College of Chemistry, Jilin University, 2699 Qianjin Street, Changchun 130012, China

[‡]College of Pharmacy, The Ohio State University, 500 W 12th Avenue, Columbus 43210, United States

ABSTRACT: A series of thiophene derivatives were synthesized by functionalization of 2,3-fused thiophene scaffolds. Their cytotoxicity was assessed against HeLa and Hep G2 cells. Compound 480 was identified as a promising candidate because of its low IC_{50} in HeLa (12.61 μg/mL) and Hep G2 (33.42 μg/mL) cells. The drug was loaded into folic acid (FA)-coated nanoparticles (NPs) to address its poor water solubility and to improve its selectivity for cancer cells. Compound 480 was shown to induce apoptosis by changes in mitochondrial membrane potential ($\Delta\Psi_m$) and the reactive oxygen species level. Furthermore, FA-modified NPs enhanced uptake capacity compared to unmodified controls by flow cytometry. This drug delivered in folate nanocarriers is promising for the treatment of cancers.

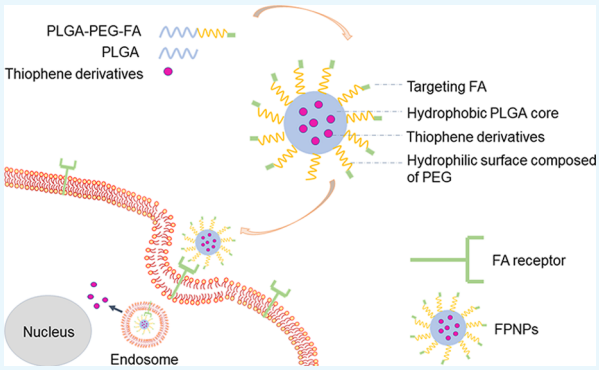

1. INTRODUCTION

Cancer is a leading cause of death in the world. Most antitumor drugs have serious side effects, which limited their application.[1−3] For example, paclitaxel is widely used in the treatment of cancer. However, its hypersensitivity reactions, hematological toxicity, neurotoxicity, and muscular toxicity limited its application.[4] The emergence of new drugs is expected to alleviate this problem. Thiophene constitutes a five-membered heterocyclic scaffold and has attracted much attention because of their presence in some marketed drugs,[5,6] including NSAID, antiasthma, diuretic, antihistaminic, and anticancer drugs.[7,8] We have synthesized a series of thiophene derivatives.[5] However, poor water solubility and severe effects have restricted their application. In fact, because of thiophene-associated hepatotoxicity, many thiophene-containing drugs have been removed from the drug market. A targeted drug delivery system may be able to address these issues.

Nanocarriers offer major advantages containing the ability to avoid multidrug resistance[9] and the enhanced permeability and retention effect in cancer therapeutics.[10,11] Nanoparticles (NPs) can also achieve sustained release of drugs and targeting effect to cancer cells by attaching targeting molecules that bind to specific receptors on the cancer cell surface,[12] such as arginine−glycine−aspartic acid, transferrin, and vitamin folate (FA).[13,14]

FA has high affinity with folate receptors (FRs), which are overexpressed in many cancer cells including breast, colorectal, ovarian, brain, and lung cancer,[14,15] while their expression in normal cells is low.[16−18] The difference can be exploited to realize the targeting of cancer cells.

Herein, thiophene derivatives were evaluated and screened for cytotoxicity, and a drug candidate compound 480 was loaded into poly(lactic-*co*-glycolic acid) (PLGA) nanocarriers coated with FA to achieve targeting to cancer cells.[19]

2. RESULTS AND DISCUSSION

2.1. Cytotoxicity of Thiophene Derivatives. A series of thiophene derivatives were synthesized, as shown in Figure 1, and analyzed for cytotoxicity. As shown in Figure 2A, paclitaxel was used as a control, and compounds 471 and 480 had high cytotoxicity with IC_{50} of 23.79 and 33.42 μg/mL, respectively, against HeLa cells. For Hep G2 cells, the IC_{50} values were 13.34 and 12.61 μg/mL. Moreover, as depicted in Figure 2B, they were all cytotoxic against normal cells (HEK-293T) at a concentration of 20 μg/mL, which suggested that they had no ability to specifically recognize cancer cells. In addition, we measured their solubility in water and concluded that the solubility of compound 480 is 25 μg/mL, whereas compound 471 is insoluble in water. Therefore, compound 480 was chosen for further evaluation.

2.2. Characterization of NPs-480. Compound 480 had high cytotoxicity but had poor water solubility (20 μg/mL) and lacked tumor cell selectivity. To address these issues, we designed and prepared targeted NPs loaded with compound 480 by a single-emulsion method and decorated FA as a targeting ligand. The NPs were prepared by an oil-in-water

Received: February 27, 2019
Accepted: April 30, 2019
Published: May 22, 2019

DOI: 10.1021/acsomega.9b00554
ACS Omega 2019, 4, 8874−8880

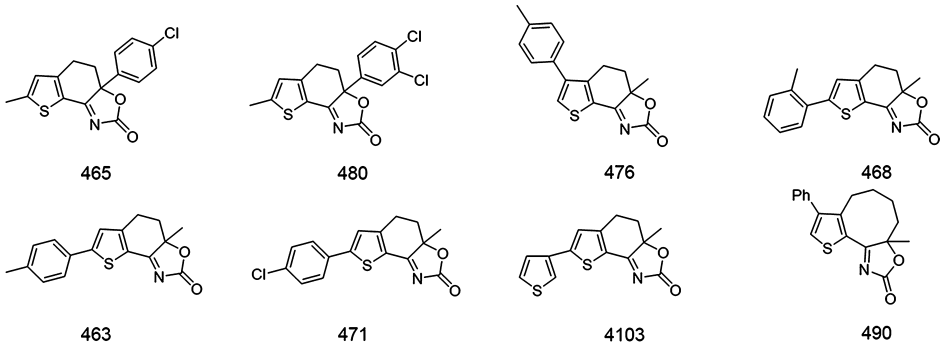

Figure 1. Chemical structure of compounds.

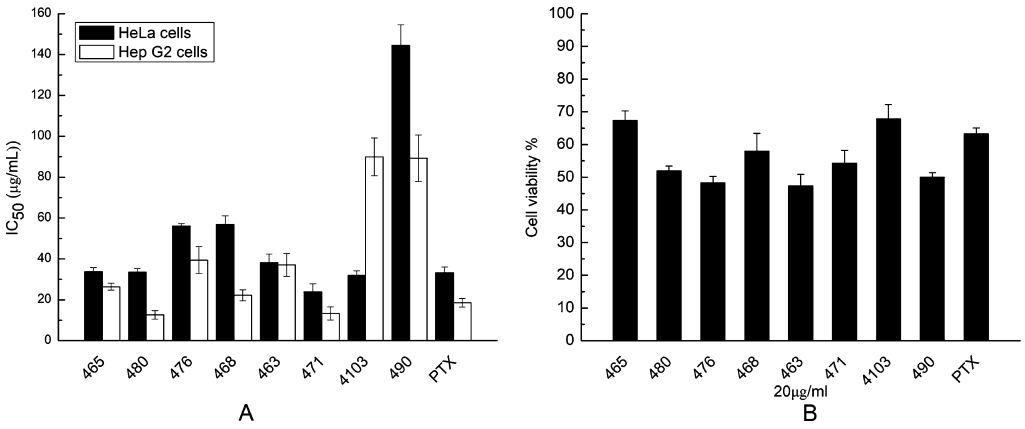

Figure 2. Cytotoxicity of thiophene derivatives. (A) IC_{50} of the thiophene derivatives against HeLa and Hep G2 cell lines. (B) Cytotoxicity of 20 μg/mL derivatives in HEK-293T cells. Data represent the mean ± SD (n = 6).

emulsion method for its high solubility of 15 mg/mL in dichloromethane. Characteristics of the NPs including particle size, polydispersity index (PDI), drug loading (DL), and entrapment efficiency (EE) are shown in Table 1. The

Table 1. Characteristics of NPs[a]

	size (nm)	PDI	EE (%)
PNPs-480	163.9 ± 7.067	0.082 ± 0.013	96.73 ± 1.89
FPNPs-480	172.4 ± 2.052	0.144 ± 0.036	94.64 ± 0.73

[a]Data represent the mean ± SD (n = 3).

diameter of folate modified PLGA nanoparticles (FPNPs) was 172.4 ± 2.052 nm, with a PDI of 0.144 ± 0.036, similar to PLGA nanoparticles (PNPs) (163.9 ± 7.067 nm), which indicates narrow particle size distribution. As shown in Figure 3, the scanning electron microscopy (SEM) image revealed that FPNPs-480 were monodisperse spheres with smooth shapes. The mean diameter was smaller than that determined by dynamic light scattering (DLS).

We used high-performance liquid chromatography (HPLC) to measure the DL and calculated the EE. The loading efficiencies of compound 480 in FPNPs-480 and PNPs-480 were 94.64 and 96.73% w/w, respectively.

2.3. Colloidal Stability of NPs. NPs incubated in different media were evaluated for their stability by size and PDI analyses. As shown in Figure 4A,B, particle size and PDI at 4 °C did not change much within a week in deionized water and phosphate-buffered saline (PBS) (pH 7.4) but increased after the fifth day in PBS with 10% fetal bovine serum (FBS). Figure 4C,D shows the stability of NPs incubated at 37 °C, which

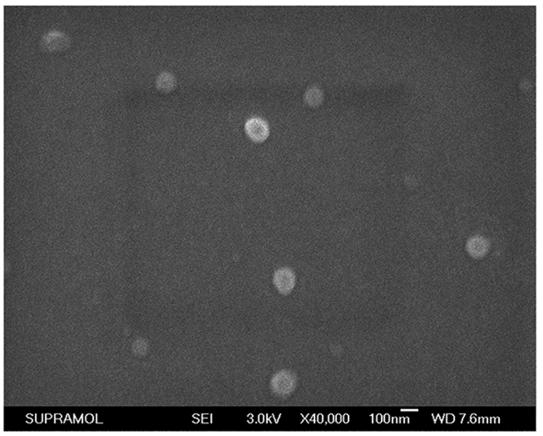

Figure 3. SEM image of FPNPs-480.

suggested that NPs were stable in deionized water and began to aggregate slightly from day 6 in PBS, which indicated that the NPs were relatively stable. In addition, there was a rapid increase from day 4 in PBS with 10% FBS, but this would not affect the results in vivo and in vitro cell experiments because of their rapid distribution after intravenous injection.

2.4. In Vitro Release. The in vitro release profiles of PNPs-480 and FPNPs-480 incubated in PBS with 40% ethanol for 2 days are shown in Figure 5. The release profiles of PNPs and FPNPs were similar, with a cumulative release of 80 and 86% after 48 h, respectively. The release rate of FPNPs was similar to PNPs, and they all showed a sustained release pattern.

DOI: 10.1021/acsomega.9b00554
ACS Omega 2019, 4, 8874−8880

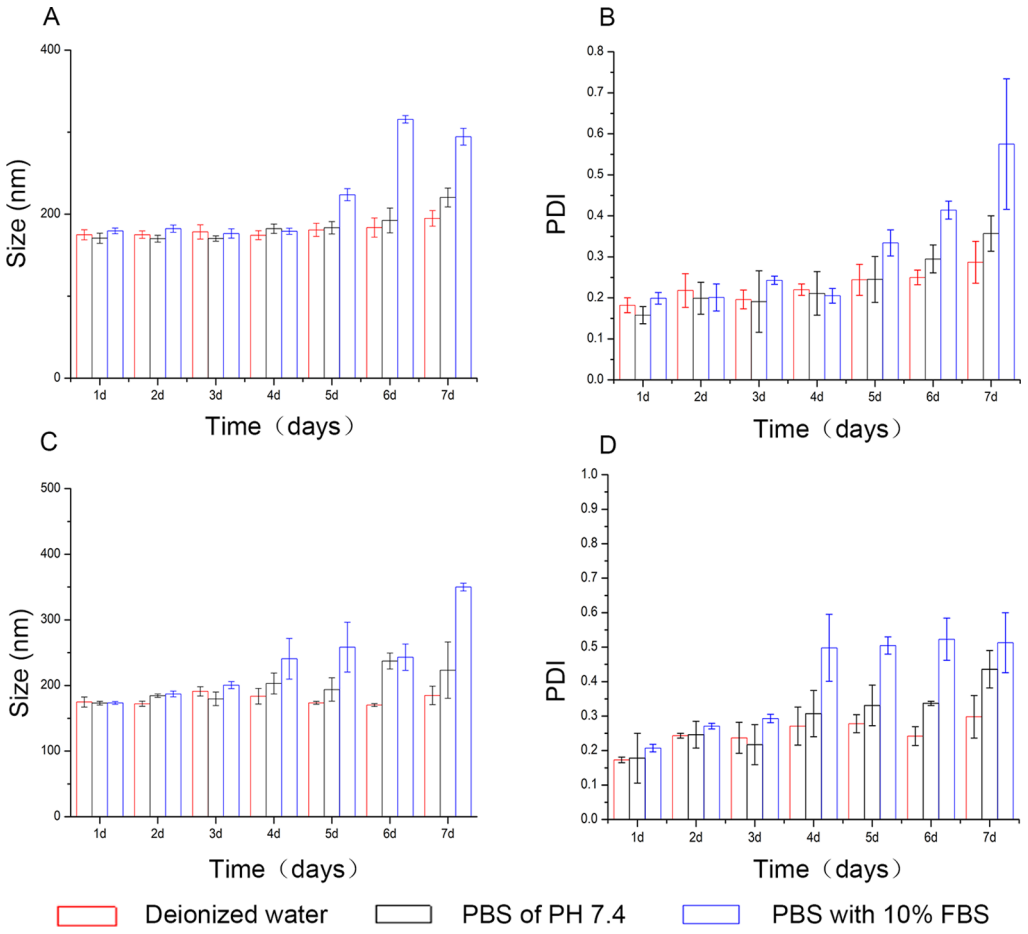

Figure 4. Size and PDI stability of FPNPs-480. FPNPs-480 stored in three various media at 4 °C (A,B) and 37 °C (C,D). Values are mean ± SD (n = 3).

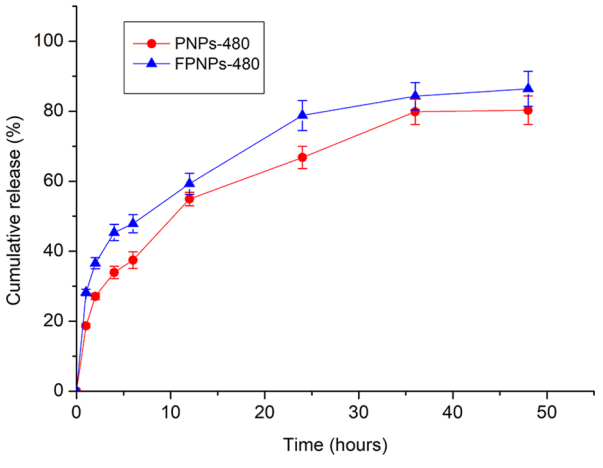

Figure 5. In vitro release compound 480 profiles using the dialysis method. PNPs-480 and FPNPs-480 were incubated in PBS containing 40% (v/v) ethanol at 37 °C. Values are mean ± SD (n = 3).

2.5. Cytotoxicity Assays. The cytotoxic effects of blank FPNPs, free drugs, PNPs-480, and FPNPs-480 were measured by the 3-(4,5-dimethylthiazol-2-yl)-2,5-diphenyltetrazolium bromide (MTT) assay. As depicted in Figure 6A, blank FPNPs had no significant cytotoxic effect on cells. Free drugs acted fast, and they showed stronger cytotoxicity than PNPs-480 and FPNPs-480. This could be due to the attenuated release of the drug from the NPs. Both PNPs-480 and FPNPs-480 displayed time-dependent cytotoxicity in 72 h. In Figure 6B, a significant difference in cell viability was found between the FPNPs-480-treated group and the PNPs-480-treated group at 24 h ($P < 0.05$) and 48 h ($P < 0.01$) against HeLa cells, respectively. A difference in cell viability was found in Hep G2 cells at 48 h ($P < 0.05$) as exhibited in Figure 6C. In short, FPNPs-480 exhibited higher cytotoxicity than PNPs-480, which was likely due to the FR targeting. The cytotoxicity of NPs in normal cells (HEK-293T) is given in Figure 6D. No significant difference in cytotoxicity was observed between the FPNPs-480- and the PNPs-480-treated groups. This indicated that the FA-mediated pathway enhanced the uptake of cancer cells with a high level of FRs.

2.6. Mitochondrial Membrane Potential Assay. Apoptosis induction by compound 480 was assessed through $\Delta\Psi_m$ using the 5,50,6,60-tetrachloro-1,10,3,30-tetraethyl-imidacarbocyanine iodide (JC-1) fluorescent probe in HeLa and Hep G2 cells. As shown in Figure 7, the green fluorescence intensity of the three groups increased to varying degrees, indicating the apoptosis induction by compound 480. Interestingly, FPNPs-480-treated cells showed much lower red−green fluorescence ratio than the cells treated with PNPs-480 because of FR targeting.

2.7. Assessment of the Generation Level of ROS. Intracellular reactive oxygen species (ROS) level was measured using the fluorescent dye 2′-7′-dichlorodihydrofluorescein diacetate (DCFH-DA). ROS is involved in cell growth, proliferation, and apoptosis. Elevated high levels of ROS can

DOI: 10.1021/acsomega.9b00554
ACS Omega 2019, 4, 8874−8880

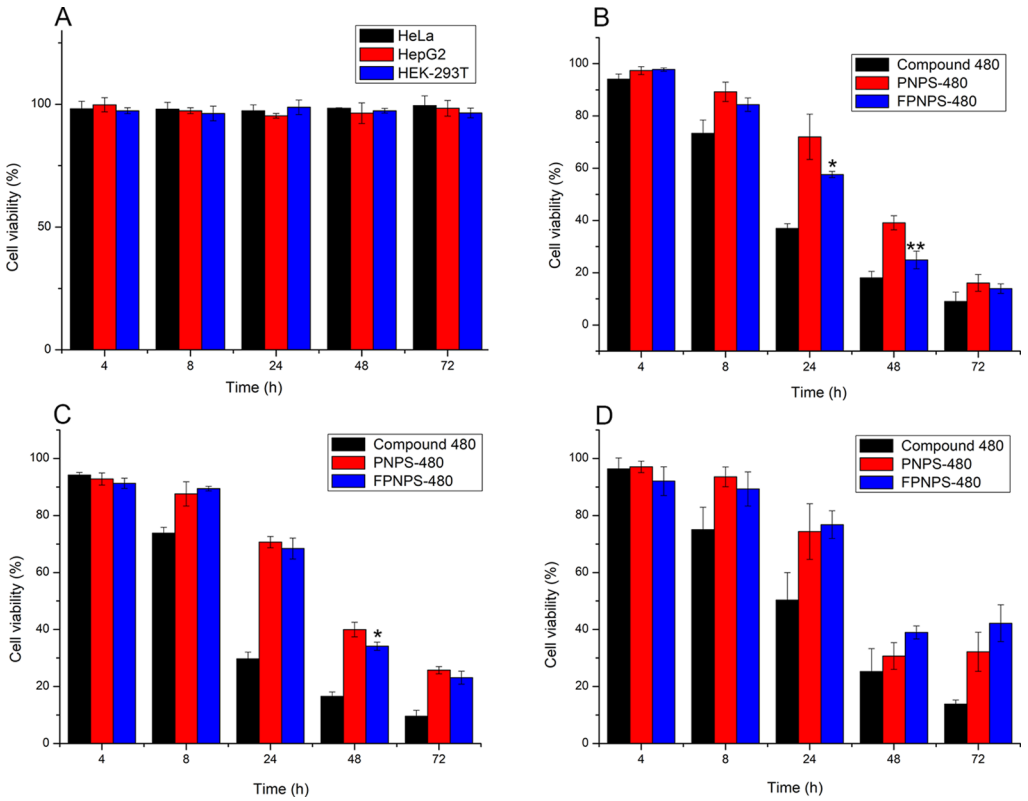

Figure 6. Cytotoxicity of NPs. HeLa, Hep G2, and HEK-293T cells were treated with blank FPNPs (A). HeLa cells (B), Hep G2 cells (C), and HEK-293T cells (D) were treated with free drugs, PNPS-480, and FPNPs-480 with different exposure times. Data represent the mean ± standard deviation (n = 3).

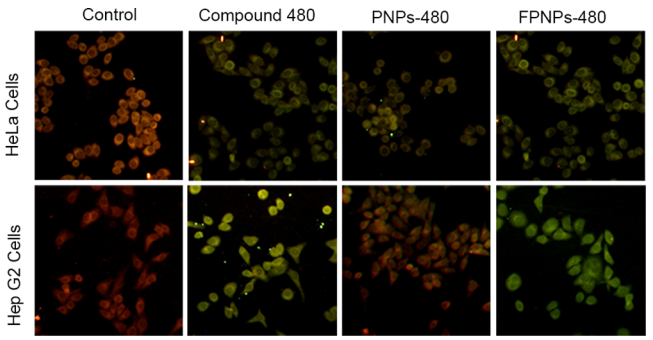

Figure 7. Effect of $\Delta\Psi_m$. Cells were treated with free drugs, PNPs-480, and FPNPs-480, and $\Delta\Psi_m$ were reflected by the intensity of red and green fluorescence. Photograph shows the merged image of JC-1 red and green.

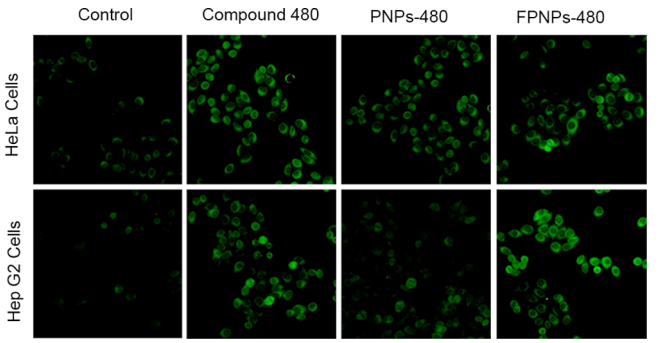

Figure 8. ROS level detection. Effect on the ROS level against cancer cells of free drugs, PNPs, and FPNPs reflected by the intensity of green fluorescence image.

make mitochondrial dysfunction promote cell apoptosis. The ROS in the cell can oxidize nonfluorescent DCFH to green fluorescent DCF. The fluorescence intensity is proportional to the level of ROS.

The levels of ROS produced by the two cancer cells treated with compound 480, PNPs-480, and FPNPs-480 are presented in Figure 8. All of them were capable of making cells apoptotic. Among them, FPNPs-480 had the highest green fluorescence intensity compared with PNPs-480, which was likely due to their FR-targeting capability.

2.8. In Vitro Cellular Uptake. To investigate the role of FR in the uptake of NPs against HeLa cells, PNPs and FPNPs were labeled with rhodamine B.

As shown in Figure 9, HeLa cells had higher red fluorescence intensity in the group treated with rhodamine B-labeled FPNP group than that treated with the PNP group. These results indicated that FA-modified NPs can enhance cellular uptake.

Flow cytometry was performed for measuring the uptake of rhodamine-labeled PNPs and FPNPs under the same culture condition. The results are shown in Figure 10. PNP- and FPNP-treated groups had very significant differences compared with control. The fluorescence intensity of cells with high FPNP uptake was 1.43 times than that of cells treated with the PNP group ($p < 0.01$). This indicated that FR targeting mediated more efficient uptake in vitro, which was consistent with confocal results.

DOI: 10.1021/acsomega.9b00554
ACS Omega 2019, 4, 8874−8880

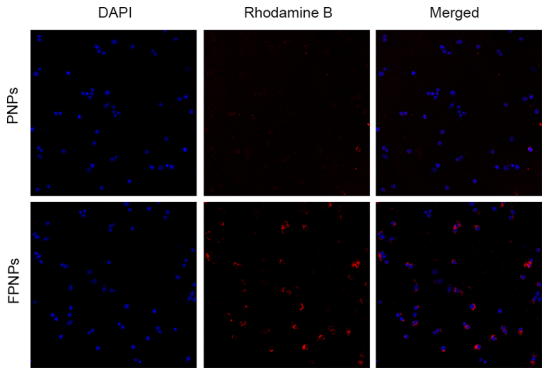

Figure 9. Intracellular uptake of NPs. Confocal images show intracellular uptake of rhodamine B-labeled PNPs and FPNPs against HeLa cells.

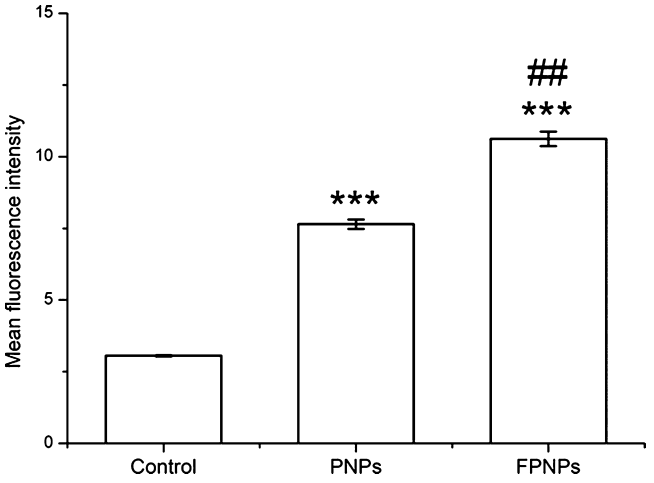

Figure 10. Cellular uptake of NPs. Cells were treated with the rhodamine B-labeled NPs. Values are mean ± SD (n = 3, ***P < 0.001 vs control, $^{\#\#}p$ < 0.01 vs PNPs).

3. CONCLUSIONS

In this study, we synthesized a series of thiophene derivatives. The antitumor activity of these compounds was then evaluated by the cytotoxicity assay. Compound 480 was identified as a promising anticancer agent for having higher antitumor activity with low IC_{50} in HeLa (12.61 μg/mL) and HepG2 (33.42 μg/mL), which was much lower than paclitaxel (Figure 2) under the same experimental conditions. In this study, FR-targeting NPs were then used to address their poor water solubility and nonspecificity. The nanocarriers showed a desirable mean diameter with narrow size distribution, high encapsulation efficiency, and excellent serum stability. Compound 480 can induce a change in $\Delta\Psi_m$ and ROS generation. Our results verified that FA-modified NPs had enhanced uptake capacity compared to unmodified controls. In short, FPNPs-480 showed an excellent therapeutic effect on cancer. It improved the solubility of drugs and promoted tumor uptake through the FR. Its mechanism of action and its application in cancer therapy warrant further investigation.

4. EXPERIMENTAL SECTION

4.1. Materials. PLGA 5050 1.5A was supplied by Boehringer Ingelheim Pharma (Ingelheim am Rhein, Germany). NH_2−PEG−NH_2 [molecular weight (MW) 5000 Da] was obtained from Yare Biotechnology (Shanghai, China). FA and MTT were obtained from Yuanye Biotechnology (Shanghai, China). Polyvinyl alcohol (87−89% hydrolyzed, MW 13 000−23 000 Da) and JC-1 were purchased from Sigma-Aldrich (St Louis, MO, USA). DCFH-DA, a fluorescent dye, was obtained from Nanjing Jiancheng Bioengineering Institute (Nanjing, China). 4′,6-Diamidino-2-phenylindole (DAPI) was obtained from Beyotime Institute of Biotechnology (Haimen, China). Rhodamine B was obtained from Sinopharm Chemical Reagent (Shanghai, China). HeLa, Hep G2, and HEK-293T cell lines were purchased from American Type Culture Collection (ATCC). Acetonitrile was purchased from Thermo Fisher Scientific.

4.2. Cell Culture. HeLa, Hep G2, and HEK-293T cells were cultured in Dulbecco's modified Eagle's medium (DMEM) containing 10% FBS, 100 units/mL penicillin, and 0.1 mg/mL streptomycin under humidified conditions at 37 °C with 5% CO_2.

4.3. MTT Assay. Three cell lines: HeLa, Hep G2, and HEK-293T, were used to evaluate cytotoxicity. Briefly, these compounds (Figure 1) were dissolved in 5% ethanol and then diluted to different concentrations in DMEM. Cells were seeded in a 96-well plate for 24 h. Then, the medium was replaced with a medium containing various concentrations of compounds for additional 24 h. Subsequently, after a 4 h incubation because MTT was added, the medium was discarded and dimethyl sulfoxide (DMSO) was added. Absorbance was measured at 490 nm by a microplate reader. Paclitaxel and basic medium containing 5% ethanol were used as positive and negative controls, respectively.

4.4. Preparation of NPs. FA-PEG-PLGA was synthesized as described previously.[20,21] FPNPS-480 was prepared as follows: PLGA (28.5 mg), PLGA-PEG-FA (9.5 mg), and compound 480 (1.22 mg, 3.0 wt %) were dissolved in 4 mL of chloroform/acetone (1:1 v/v). The solution was injected into 8 mL of 1% (w/v) poly(vinyl alcohol) under sonication in an ice bath over 30 s at 200 W with 15 pulses of 1 s duration and sonicated for additional 2 min. The resulting emulsion was then dispersed in 15 mL of deionized water and evaporated for 4 h at room temperature to remove organic solvent. PNPS-480 was prepared using the same procedure except for replacement of PLGA-PEG-FA with PLGA. In addition, rhodamine B-loaded NPs were prepared for uptake experiments in order to facilitate detection. The obtained NPs were pelleted by centrifugation (20 000 rpm, 15 min), washed three times, resuspended in 1 mL of deionized water, lyophilized, and stored at 4 °C.

4.5. Characterization of NPs. Particle size and PDI of NPs were measured using DLS (Zetasizer Nano ZS90, Malvern Instruments, Malvern, UK). Morphological characteristics of NPs were observed by SEM (JXA-840, JEOL, Tokyo, Japan). Drops of NPs were added to the surface of the silicon wafer and dried for further observation by SEM.

The loading capacity and EE were determined using an HPLC (Waters Corp, Milford, MA, USA) system equipped with an Agilent XDB-C18 column (4.6 mm × 250 mm, 5 μm) at 300 nm. Briefly, NPs were destroyed by acetonitrile on vortex for releasing the compound, and then the mobile phase (60% of acetonitrile) was added to extract the compound. Then compound 480 was analyzed by HPLC. DL and EE were calculated according to the following formula

$$\mathrm{DL}\ (\%) = \frac{\text{weight of drug in NPs}}{\text{weight of drug in NPs}} \times 100\%$$

DOI: 10.1021/acsomega.9b00554
ACS Omega 2019, 4, 8874−8880

$$\text{EE}\ (\%) = \frac{\text{actual drug loading}}{\text{theoretical drug loading}} \times 100\%$$

4.6. Colloidal Stability of NPs. NPs suspended in deionized water, PBS (0.1 M, pH 7.4), and PBS with 10% FBS at 37 and 4 °C, respectively, were analyzed by DLS at predetermined time points to evaluate their sizes and PDI.

4.7. In Vitro Release. Dialysis method was used to measure in vitro release kinetics for PNPs-480 and FPNPs-480.[22] Dispersions of PNPs-480 and FPNPs-480 corresponding to 1 mg of compound 480 were loaded into dialysis bags (MWCO 7 kD), immersed in 50 mL PBS-40% ethanol, and incubated in a water shaker at 37 °C and 100 rpm.[23] At fixed time points, 5 mL of samples were withdrawn and replaced with equal amounts of fresh dialysis medium. The cumulative percentage of drug release was determined using HPLC.

4.8. Cytotoxicity Assays. The cytotoxic effect of compound 480, PNPs-480, and FPNPs-480 against HeLa, Hep G2, and HEK-293T cells was evaluated by the MTT method, respectively. Cells were plated at a density of 6000 cells/well in 96-well plates and incubated for 24 h. Then, the medium was replaced with fresh medium containing free drugs, PNPs, and FPNPs. At predetermined time points, MTT was added. After incubating for 4 h, absorbance was measured on a microplate reader.

4.9. Mitochondrial Membrane Potential ($\Delta\Psi_m$) Assessment. $\Delta\Psi_m$ was used to determine cellular apoptosis because the loss of $\Delta\Psi_m$ is an early event in the apoptotic process. JC-1 is a fluorescence probe widely applied to detect $\Delta\Psi_m$. At high $\Delta\Psi_m$, JC-1 accumulates in the mitochondrial matrix and forms a polymer that produces red fluorescence. At low $\Delta\Psi_m$, JC-1 exists as a monomer and produces green fluorescence. The difference in the ratio between green and red fluorescence was viewed by a fluorescence inverted microscope.

The cells were cultured for 24 h. Then, the medium was displaced with a new medium including compound 480, PNPs-480, or FPNPs-480. After 12 h, the cells were washed with PBS and incubated with the JC-1 dye in PBS (0.01 M, pH 7.4) for 10 min in the dark and then inspected with a fluorescent inverted microscope.

4.10. Evaluation of the ROS Level. Cells were plated in six-well plates at a density of 2×10^5 per well, incubated for 24 h, and then treated with fresh medium containing free drugs, PNPs-480, or FPNPs-480 for 12 h. Then, the cells were incubated with 10 μM DCFH-DA in PBS (pH 7.4) for 10 min in darkness. Subsequently, the cells were washed and imaged with an inverted microscope.

4.11. In Vitro Cellular Uptake Studies. Uptake of PNPs and FPNPs by HeLa cells was evaluated. Cells were incubated for 24 h and treated with rhodamine B-loaded NPs for 4 h. Then, cells were washed with PBS (0.01 M, pH 7.4) and fixed in 4% formaldehyde. After 10 min, nuclei were stained with DAPI according to protocols from the supplier. Uptake of cells was visualized by a confocal mcroscope (LSM710, Carl Zeiss, Jena, Germany).

HeLa Cells were cultured for 24 h. The medium was discarded and changed into medium including rhodamine-labeled NPs. After incubation for 4 h, the cells were washed three times with PBS (0.01 M, pH 7.4), released with 100 μL trypsin, and then analyzed by an EPICS XL flow cytometer from Beckman Coulter (Brea, CA, USA). Ten thousand cells were analyzed in triplicates for each group.

4.12. Statistical Analysis. Data are shown as mean ± SD. Results were analyzed using Student's *t*-test. *P* values < 0.05 were regarded as statistically significant. All experiments were performed in triplicate.

AUTHOR INFORMATION

Corresponding Authors

*E-mail: liyouxin@jlu.edu.cn (Y.L.).
*E-mail: tenglesheng@jlu.edu.cn (L.T.).

ORCID

Menghui Zhao: 0000-0002-2829-9126
Robert J. Lee: 0000-0002-5981-5867
Weiwei Liao: 0000-0001-6225-4258
Lesheng Teng: 0000-0003-1623-5384

Notes

The authors declare no competing financial interest.

ACKNOWLEDGMENTS

This research was supported by Jilin Province Science and Technology Development Program (no. 20180101269JC) and the Graduate Innovation Fund of Jilin University (RA-ART-12-2018-010555).

ABBREVIATIONS

PLGA, poly(lactic-*co*-glycolic acid); FA, folate; FPNPs, folate-modified nanoparticles

REFERENCES

(1) Liang, H.-F.; Chen, C.-T.; Chen, S.-C.; Kulkarni, A. R.; Chiu, Y.-L.; Chen, M.-C.; Sung, H.-W. Paclitaxel-loaded poly(gamma-glutamic acid)-poly(lactide) nanoparticles as a targeted drug delivery system for the treatment of liver cancer. *Biomaterials* **2006**, *27*, 2051−2059.

(2) Danhier, F.; Feron, O.; Préat, V. To exploit the tumor microenvironment: Passive and active tumor targeting of nanocarriers for anti-cancer drug delivery. *J. Controlled Release* **2010**, *148*, 135−146.

(3) Cho, K.; Wang, X.; Nie, S.; Chen, Z.; Shin, D. M. Therapeutic nanoparticles for drug delivery in cancer. *Clin. Cancer Res.* **2008**, *14*, 1310−1316.

(4) Sakamoto, J.; Matsui, T.; Kodera, Y. Paclitaxel chemotherapy for the treatment of gastric cancer. *Gastric Cancer* **2009**, *12*, 69−78.

(5) Zhao, L.; Liao, W.-W. Pd-Catalyzed intramolecular C−H addition to the cyano-group: construction of functionalized 2,3-fused thiophene scaffolds. *Org. Chem. Front.* **2018**, *5*, 801−805.

(6) Mohareb, R. M.; Abdallah, A. E. M.; Abdelaziz, M. A. New approaches for the synthesis of pyrazole, thiophene, thieno[2,3-b]pyridine, and thiazole derivatives together with their anti-tumor evaluations. *Med. Chem. Res.* **2013**, *23*, 564−579.

(7) Gramec, D.; Mašič, L. P.; Sollner Dolenc, M. Bioactivation potential of thiophene-containing drugs. *Chem. Res. Toxicol.* **2014**, *27*, 1344−1358.

(8) Joshi, E. M.; Heasley, B. H.; Chordia, M. D.; Macdonald, T. L. In Vitro Metabolism of 2-Acetylbenzothiophene: Relevance to Zileuton Hepatotoxicity†. *Chem. Res. Toxicol.* **2004**, *17*, 137−143.

(9) Sudimack, J.; Lee, R. J. Targeted drug delivery via the folate receptor. *Adv. Drug Delivery Rev.* **2000**, *41*, 147−162.

(10) Maeda, H.; Wu, J.; Sawa, T.; Matsumura, Y.; Hori, K. Tumor vascular permeability and the EPR effect in macromolecular therapeutics: a review. *J. Controlled Release* **2000**, *65*, 271−284.

(11) Xu, L.; Xu, S.; Wang, H.; Zhang, J.; Chen, Z.; Pan, L.; Wang, J.; Wei, X.; Xie, H.; Zhou, L.; Zheng, S.; Xu, X. Enhancing the Efficacy and Safety of Doxorubicin against Hepatocellular Carcinoma through a Modular Assembly Approach: The Combination of Polymeric Prodrug Design, Nanoparticle Encapsulation, and Cancer Cell-

DOI: 10.1021/acsomega.9b00554
ACS Omega 2019, 4, 8874−8880

Specific Drug Targeting. *ACS Appl. Mater. Interfaces* **2018**, *10*, 3229−3240.
(12) Byrne, J. D.; Betancourt, T.; Brannon-Peppas, L. Active targeting schemes for nanoparticle systems in cancer therapeutics. *Adv. Drug Delivery Rev.* **2008**, *60*, 1615−1626.
(13) Peer, D.; Karp, J. M.; Hong, S.; Farokhzad, O. C.; Margalit, R.; Langer, R. Nanocarriers as an emerging platform for cancer therapy. *Nat. Nanotechnol.* **2007**, *2*, 751.
(14) Wang, J.; Wang, H.; Li, J.; Liu, Z.; Xie, H.; Wei, X.; Lu, D.; Zhuang, R.; Xu, X.; Zheng, S. iRGD-Decorated Polymeric Nanoparticles for the Efficient Delivery of Vandetanib to Hepatocellular Carcinoma: Preparation and in Vitro and in Vivo Evaluation. *ACS Appl. Mater. Interfaces* **2016**, *8*, 19228−19237.
(15) Parker, N.; Turk, M. J.; Westrick, E.; Lewis, J. D.; Low, P. S.; Leamon, C. P. Folate receptor expression in carcinomas and normal tissues determined by a quantitative radioligand binding assay. *Anal. Biochem.* **2005**, *338*, 284−293.
(16) Soleymani, J.; Hasanzadeh, M.; Somi, M. H.; Shadjou, N.; Jouyban, A. Probing the specific binding of folic acid to folate receptor using amino-functionalized mesoporous silica nanoparticles for differentiation of MCF 7 tumoral cells from MCF 10A. *Biosens. Bioelectron.* **2018**, *115*, 61−69.
(17) Leamon, C. P.; Low, P. S. Folate-mediated targeting: from diagnostics to drug and gene delivery. *Drug Discovery Today* **2001**, *6*, 44−51.
(18) Leamon, C.; Reddy, J. A. Folate-targeted chemotherapy. *Adv. Drug Delivery Rev.* **2004**, *56*, 1127−1141.
(19) Danhier, F.; Ansorena, E.; Silva, J. M.; Coco, R.; Le Breton, A.; Préat, V. PLGA-based nanoparticles: an overview of biomedical applications. *J. Controlled Release* **2012**, *161*, 505−522.
(20) Chen, J.; Li, S.; Shen, Q. Folic acid and cell-penetrating peptide conjugated PLGA−PEG bifunctional nanoparticles for vincristine sulfate delivery. *Eur. J. Pharm. Sci.* **2012**, *47*, 430−443.
(21) Yoo, H. S.; Park, T. G. Folate receptor targeted biodegradable polymeric doxorubicin micelles. *J. Controlled Release* **2004**, *96*, 273−283.
(22) Dora, C. P.; Kushwah, V.; Katiyar, S. S.; Kumar, P.; Pillay, V.; Suresh, S.; Jain, S. Improved oral bioavailability and therapeutic efficacy of erlotinib through molecular complexation with phospholipid. *Int. J. Pharm.* **2017**, *534*, 1−13.
(23) Li, F.; Mei, H.; Gao, Y.; Xie, X.; Nie, H.; Li, T.; Zhang, H.; Jia, L. Co-delivery of oxygen and erlotinib by aptamer-modified liposomal complexes to reverse hypoxia-induced drug resistance in lung cancer. *Biomaterials* **2017**, *145*, 56−71.

DOI: 10.1021/acsomega.9b00554
ACS Omega 2019, 4, 8874−8880